J. Fluid Mech. (1993), *vol.* 251, *pp.* 173–201
Copyright © 1993 Cambridge University Press

The near-wake of an oscillating trailing edge: mechanisms of periodic and aperiodic response

By A. LOTFY AND D. ROCKWELL

Department of Mechanical Engineering and Mechanics, 356 Packard Laboratory no. 19, Lehigh University, Bethlehem, PA 18015, USA

(Received 25 June 1991 and in revised form 18 August 1992)

This investigation addresses the unsteady wake from a blunt trailing edge subjected to controlled perturbations. The relationship between the structure of the near wake, the surface loading on the edge, and the motion of the edge is characterized by flow visualization in conjunction with velocity and pressure measurements. The response of the near wake can be classified into two general categories: a modulated wake, characterized by ordered variations in the near-wake flow structure over a number of cycles of oscillation of the trailing edge; and a phase-locked wake, whereby the near-wake structure does not change from cycle to cycle of the edge oscillation. For the modulated wake, there are large, repetitive excursions of the near-wake vortex pattern in the streamwise direction due to coexistence of the self-excited global instability of the wake and the applied excitation. These excursions can have an amplitude two orders of magnitude larger than the amplitude of the edge motion. The duration of these excursions, in relation to the cyclic motion of the trailing edge, is deterministic. For the phase-locked wake, small changes of the edge oscillation frequency produce large changes in the phase shift of the initially formed vortex from the edge. These phase shifts are due to changes in the times required for vortex formation and departure from the near wake. The corresponding mechanisms are interpreted in terms of the crucial topological features of the near wake and a phase clock concept.

1. Introduction

Shedding of vortices from a blunt trailing edge has been a subject of considerable interest over the past few decades. There are a wide variety of practical configurations that generate organized vortex streets: vanes and blades in hydraulic and turbomachinery; marine propellers; and bridge decks (Naudascher & Rockwell 1980). A detailed knowledge of the near-wake flow structure and the loading on the surface of the body is essential if one is to minimize the generation of noise and prevent the onset of structural vibration.

Investigations of the flow-induced vibration of, and vortex formation from, streamlined bodies having blunt trailing edges have been carried out by Toebes & Eagleson (1961), Wood (1971), Graham & Maull (1971), Greenway & Wood (1973), and Blake (1984). This type of vortex formation from blunt trailing edges is, in concept, very similar to the extensively investigated vortex formation from cylinders. The experimental and theoretical studies and accompanying overviews of Roshko (1954), Morkovin (1964), Bearman (1965, 1984), Berger & Wille (1972), Griffin & Ramberg (1974), Gerrard (1978), Sarpkaya (1979), Saffman & Schatzman (1982), Sreenivasan (1985), Van Atta & Gharib (1987), Ongoren & Rockwell (1988*a*, *b*), Unal & Rockwell (1988*a*, *b*), Olinger & Sreenivasan (1988), Williamson & Roshko (1988), and

Karniadakis & Triantafyllou (1989*a*, *b*) address a wide variety of issues pertinent to this general class of flows. In recent years, application of the concept of an absolute instability to the bluff-body wake has provided new insight. Koch (1985), Triantafyllou, Triantafyllou & Chryssostomodis (1986), Monkewitz & Nguyen (1987), and Monkewitz (1988) have shown that the near-wake oscillation can be interpreted as a self-excited instability. The fact that a finite streamwise lengthscale is necessary for existence of this instability is emphasized by Chomaz, Huerre & Redekopp (1988), who describe it as a global instability. An incisive overview of global instabilities is given by Huerre & Monkewitz (1990).

The overall objective of this study is to relate the structure of the near wake to the surface loading on, and the motion of, the oscillating trailing edge. Unlike most previous related investigations, the perturbation amplitude is constrained to be much smaller than the thickness of the trailing edge, in order to emphasize the quasi-linear response of the near wake. The experiment is posed to be generic to both vortex formation from cylindrical bluff bodies and from trailing edges having finite thickness. However, the use of a blunt trailing edge with sharp corners provides several well-defined conditions: the separation points do not oscillate as in the case of a circular cylinder; there is minimal oscillation of the forward stagnation point relative to that for circular cylinder; and a boundary layer under zero streamwise pressure gradient can be generated at the trailing edge, in contrast to the case of a circular cylinder where the boundary layer is subjected to strong pressure gradients around its circumference.

Excitation of a blunt trailing edge or cylinder at a frequency f_e, at or in the immediate vicinity of the inherent vortex formation frequency f_0^* produces several important effects. They include a resonant peak of the amplitude of the surface pressure or lift; an abrupt shift in the phase of this loading accompanied by a change in timing or structure of the initially formed vortex relative to the motion of the edge or cylinder. These features are reviewed by Zdravkovich (1977), Ongoren & Rockwell (1988*a*, *b*), Staubli & Rockwell (1988) and Williamson & Roshko (1988).

Only for excitation near or at $f_e/f_0^* = 1$ are the loading and vortex formation phase-locked to the edge motion. The outer boundaries of the region of phase-locked response are characterized by the onset of quasi-periodic and chaotic states, investigated from various perspectives by Sreenivasan (1985), Van Atta & Gharib (1987), Olinger & Sreenivasan (1988), and Karniadakis & Triantafyllou (1989*a*). Sreenivasan (1985) and Van Atta & Gharib (1987) demonstrate the generation of a multiplicity of spectral components. Olinger & Sreenivasan (1988) show that excitation at a value of frequency corresponding to the golden mean generates a complex spectral response; they also found a stepwise variation of f_0/f_0^*, which is the ratio of the inherent vortex formation frequencies with and without excitation; it is referred to as a devil's staircase. Karniadakis & Triantafyllou (1989*a*) numerically simulated the response of the near wake and defined the regions of f_e/f_0^* exhibiting quasi-periodic and chaotic behaviour. This wake response was interpreted in terms of multiple-peaked spectra and aperiodic phase-plane trajectories. A matter of central importance, in the context of the foregoing investigations, is the relation of possible phase modulations of the vortex formation process to the corresponding loading on the surface of the edge, and the principal parameters of the near wake that govern such modulations. If the basic mechanisms associated with this phase modulation process can be understood, it may be possible to describe the features of the aforementioned phase-locked response as a limiting case.

In summary, the principal goals of the present investigation are to: determine the character of the modulated wake at excitation frequencies away from the region where

phase-locking occurs; gain an understanding of the phase shift of vortex formation with respect to the edge motion for the phase-locked wake; and to interrelate the characteristics of the modulated and phase-locked wakes. In doing so, detailed consideration of the crucial topological features of the near wake will be essential.

2. Experimental systems and instrumentation

The experimental investigation involved a large-scale water channel, which housed a test section containing an oscillating trailing edge and its forcing system. The flow structure from, and the surface pressure field on, the oscillating trailing edge were investigated with flow visualization and velocity and pressure measurement techniques. A detailed description of the experimental arrangement and techniques is given by Lotfy (1988).

The oscillating trailing edge had a thickness T subjected to excitation frequency f_e at an amplitude η_e normalized by trailing-edge thickness T of $\eta_e/T = 0.04$. The Reynolds number based on the total effective length of the upstream plate–trailing edge system was $Re = 2.51 \times 10^4$, based on thickness T of trailing-edge $Re_T = 1400$, and based on momentum thickness θ of the boundary layer $Re_\theta = 56$.

Both dye injection and hydrogen bubble techniques were employed for flow visualization. Here the evolution of the vortex formation in the vicinity of the trailing edge is described using the hydrogen bubble technique. The platinum wire (50 μm diameter) that liberated the hydrogen bubbles was located a distance of $0.015T$ downstream of the trailing edge. Pulsation of the applied voltage allowed generation of timeline patterns. These patterns were recorded on a video system.

Velocity measurements were performed using a single-element, hot-film anemometry system. Pressure measurements involved a semiconductor-bonded strain gauge pressure transducer, mounted in such a manner as to preclude amplitude and phase distortion effects at each of the twenty-six measuring locations along the surface of the oscillating edge.

3. Overview of flow structure of modulated and phase-locked wakes

The two basic categories of near-wake structure are defined by the flow visualization of figures 1 and 2. For the first category, the vortex formation is phase-locked with respect to the motion of the trailing edge. The second category involves modulated structure of the near wake. In this case, the vortex formation is not phase locked; however, it does show highly ordered patterns of modulation over successive cycles of the edge motion.

3.1. *Phase-locked flow structure*

Phase-locked formation of vortices was found to occur in a relatively narrow frequency range $0.95 \leqslant f_e/f_0^* \leqslant 1.05$. Figure 1 shows the vortical flow structure at the maximum positive position $+\eta_{max}$ of the edge for values of frequency ratio $f_e/f_0^* = 0.95$, 1.00 and 1.05. At each value of f_e/f_0^*, three successive cycles of oscillation are illustrated. The near-wake vortex pattern is highly repeatable from cycle to cycle. In other words, the flow structure is phase locked. This locking was found to persist over a large number of oscillation cycles.

Small changes of the frequency ratio f_e/f_0^* produce large changes of the phase of formation of the upper vortex with respect to the edge position. In fact, by comparing a typical photo at $f_e/f_0^* = 1.05$ with that at 0.95, it is evident that there is a phase shift of the vortex formation process of nearly π. That is, at $f_e/f_0^* = 0.95$, vortex formation

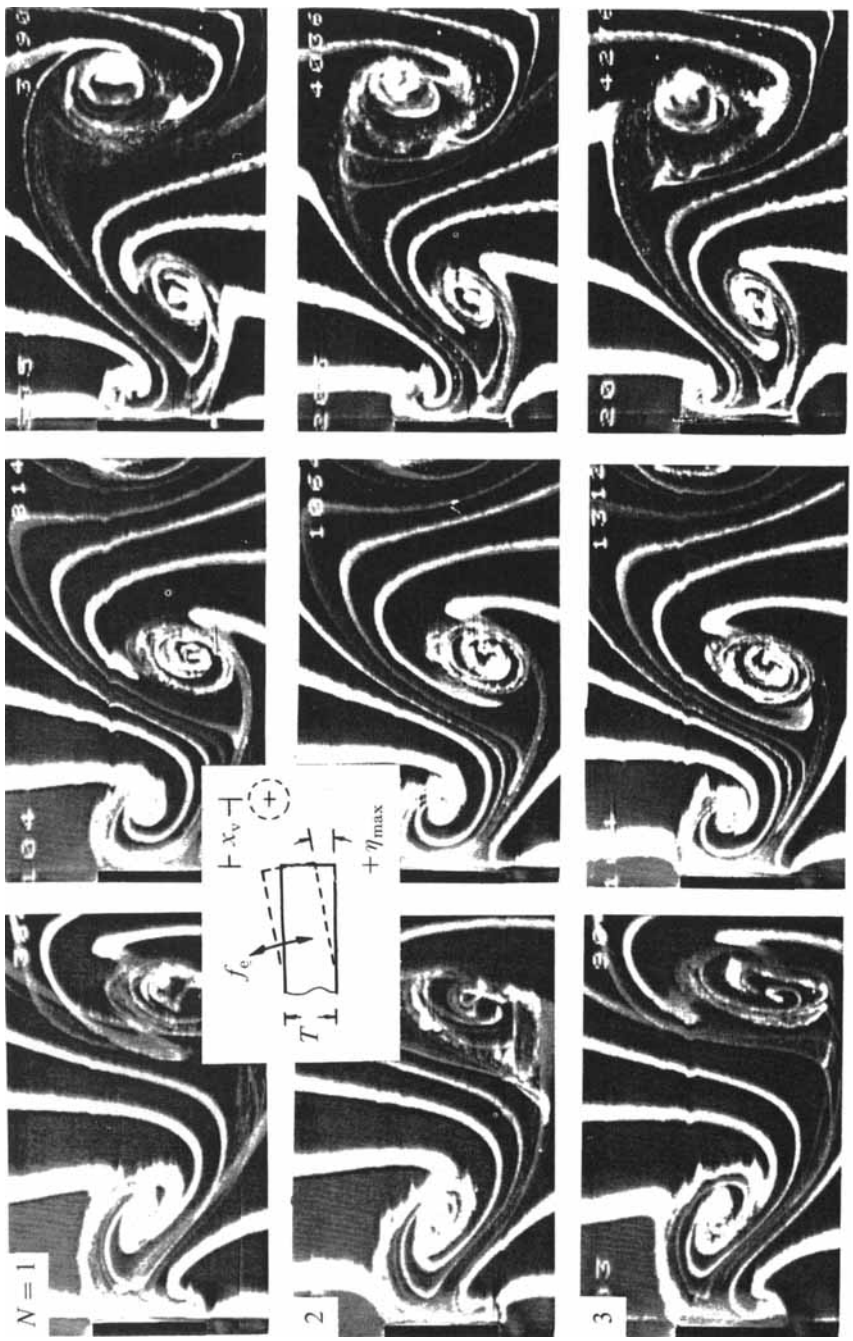

FIGURE 1. Vortex pattern for consecutive edge oscillation cycles in phase-locked region of excitation. All photos taken at maximum positive position $+\eta_{max}$ of edge. Distance x_v is streamwise displacement, T is trailing-edge thickness, and N is number of cycles of edge oscillation.

from the lower corner has just started, while at 1.05, it has just started to form from the upper corner. In addition to this substantial phase shift, it is evident that the formation length of the upper vortex moves towards the corner of the edge for increasing values of $f_e/f_0^* = 0.95, 1.0, 1.05$.

3.2. *Modulated (non phase-locked) flow structure*

Outside the relatively narrow band of excitation frequencies $0.95 \leqslant f_e/f_0^* \leqslant 1.05$, the flow structure is not phase-locked with respect to the edge motion because perturbations produced by the edge at f_e and those due to the inherent frequency f_0 of vortex shedding both exist in the near wake. To determine the nature of this modulation, the vortex shedding process was examined over ranges of excitation frequency f_e/f_0^* above and below the phase-locked range.

The flow visualization given in figures 2(*a*) and 2(*b*) shows photos taken at the instant when the trailing edge is at its maximum positive position $+\eta_{max}$. In each layout of photos, the succession of photos corresponds to successive cycles of the edge oscillation, and the total number of photos represents the number of cycles (plus one) of oscillation of the trailing edge required to complete one full cycle of modulated flow structure. Moreover, corresponding to each photo layout is a plot of x_v/T *vs.* N, in which x_v is the distance from the trailing edge to the centre of the upper U vortex, T is the trailing-edge thickness, and N is the number of oscillation cycles. The encircled data points within these plots correspond to the respective photos in the photo layout. It should be noted that plots of x_v/T *vs.* N were made over a large number of oscillation cycles in order to ascertain the periodicity; only excerpts are shown here in order to aid interpretation of the flow visualization.

For excitation at frequencies below the lower limit of phase locking, i.e. $f_e/f_0^* < 0.95$, the modulated flow structure shows the type of behaviour exhibited in figure 2(*a*), corresponding to a representative frequency ratio $f_e/f_0^* = 0.87$. The photos show that the large-scale vortex U formed from the upper side of the edge takes several cycles to form again at the same position. This is evident by comparing the first and eighth photos in figure 2(*a*) and counting the number of cycles elapsed between them. The upper vortex moves away from the trailing edge with increasing number of cycles N. This is evident not only in the flow visualization, but also in the plot of x_v/T *vs.* N. For other values of excitation frequency in the range $0.50 \leqslant f_e/f_0^* < 0.95$, the modulation pattern showed a similar trend of downstream movement of the upper U vortex with increasing N. Quantitative information on the number of cycles N for a complete modulation process is given in §7.1.

For excitation at frequencies above the upper limit of phase locking, i.e. $f_e/f_0^* > 1.05$, the flow structure exhibits a modulated behaviour analogous to that occurring at excitation below phase locking. Figure 2(*b*) represents the case of $f_e/f_0^* = 1.25$. In this case the upper vortex U moves towards the trailing edge with each successive cycle. This is shown in the successive flow visualization photos, as well as in the plot of x_v/T *vs.* N. Moreover, it is also evident that four cycles of the edge oscillation cycle are required to complete one full modulation cycle. For successively higher values of excitation frequency within the range $1.05 < f_e/f_0^* < 2.0$, there are decreases in the number of cycles of the edge motion required to form a modulation cycle. These trends are addressed quantitatively in §7.

(a)

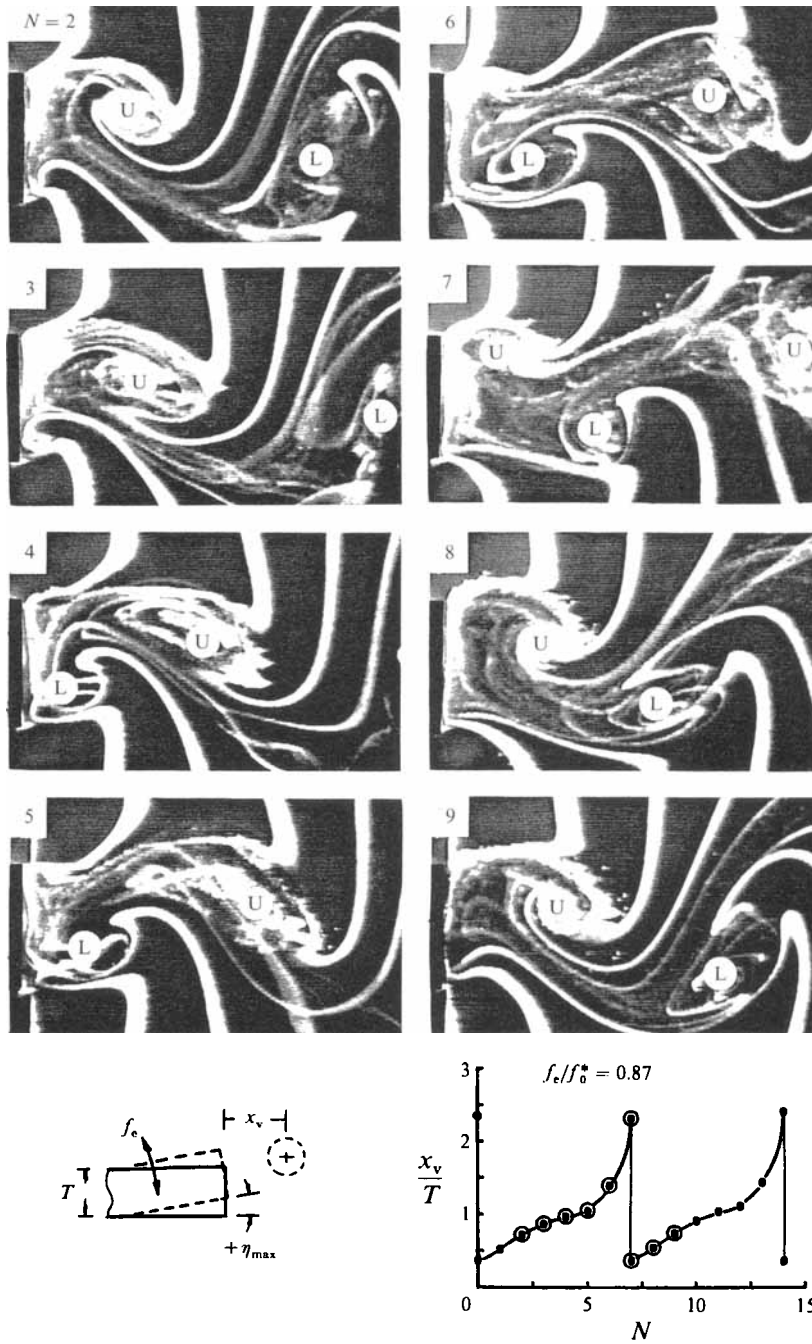

FIGURE 2(a). For caption see facing page.

4. Velocity and pressure fluctuations in the near wake

The pressure and velocity fluctuations were measured for both the stationary and oscillating trailing-edge cases. Instantaneous time signals were acquired for a large number of vortex shedding cycles; then, the corresponding time-averaged spectra were

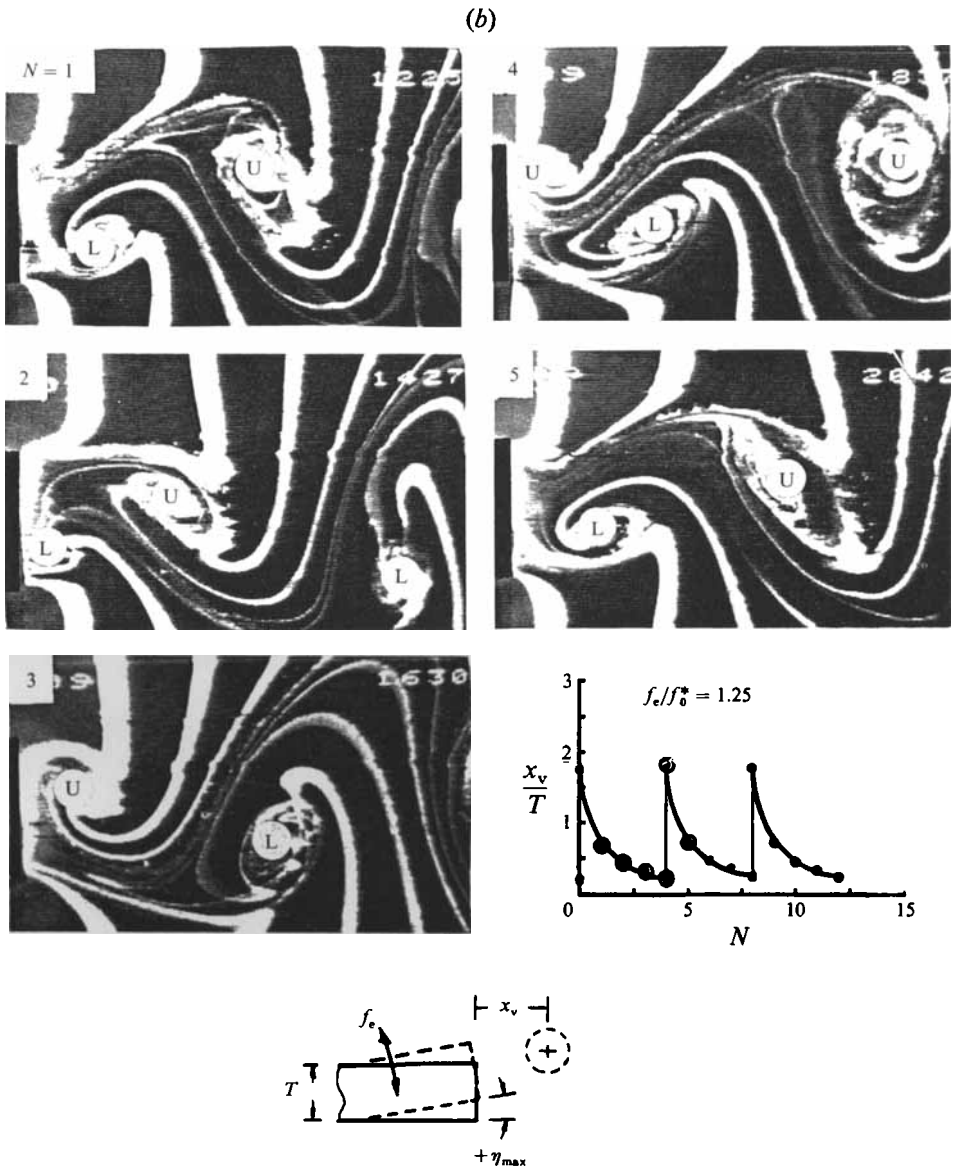

FIGURE 2. (*a*) Downstream movement of vortex pattern during one cycle of modulation. Photos represent vortex pattern for successive edge oscillation cycles at $f_e/f_0^* = 0.87$. All photos taken at maximum positive position $+\eta_{max}$ of edge. Distance x_v is streamwise displacement, T is trailing-edge thickness, and N is number of cycles of edge oscillation. (*b*) As (*a*) but for upstream movement at $f_e/f_0^* = 1.25$.

calculated. In order to analyse the effect of the edge motion on the vortex shedding process, measurements were carried out at different frequency ratios f_e/f_0^* of the edge oscillation in the ranges below, at, and above the synchronization condition $f_e/f_0^* = 1$.

4.1. *Instantaneous velocity and pressure*

Figure 3 shows a representative history of the near-wake velocity fluctuation, taken at a value of excitation frequency $f_e/f_0^* = 0.90$. The upper plot is the instantaneous time trace of the velocity fluctuation $\tilde{u}(t)$, the middle plot is the instantaneous edge

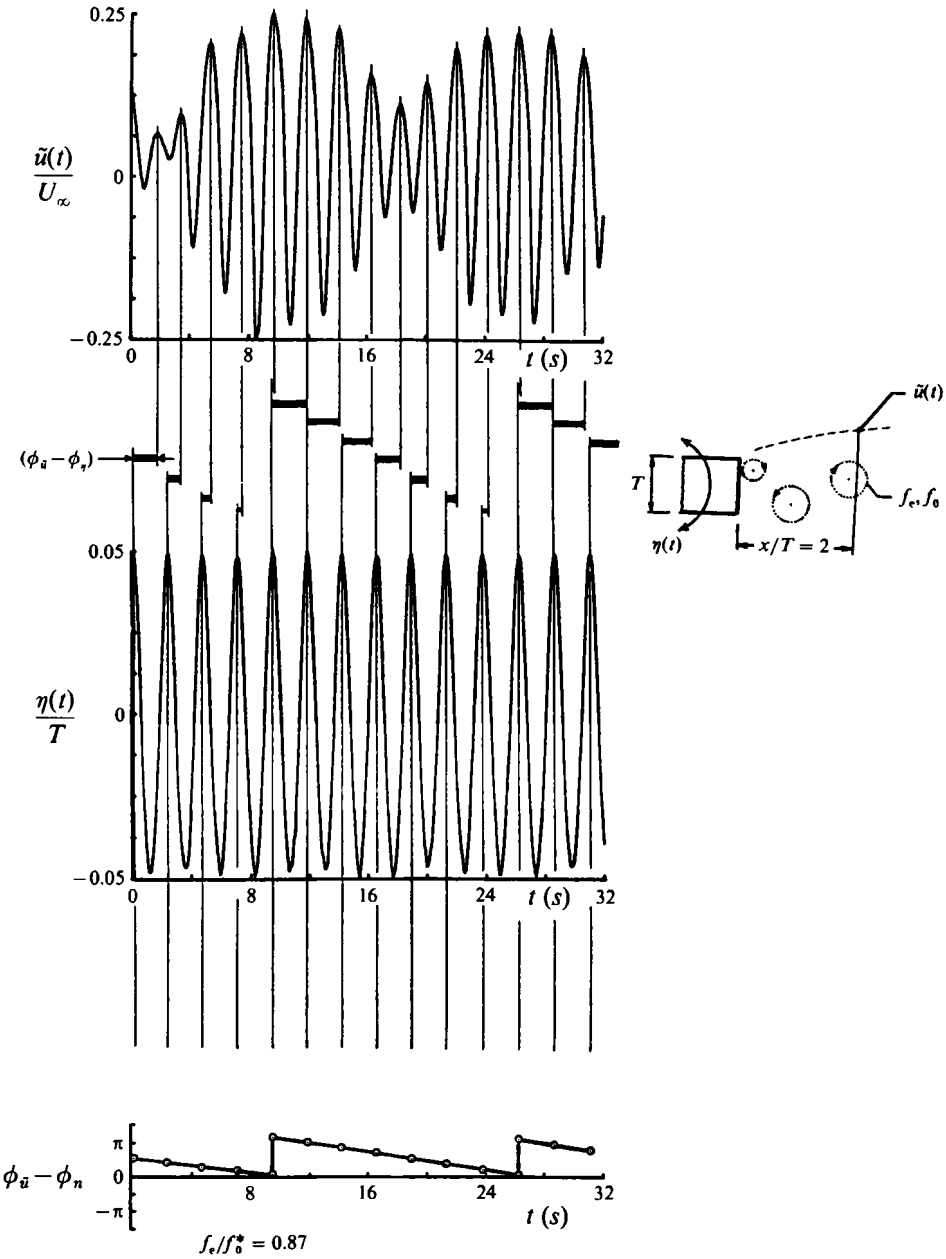

FIGURE 3. Modulated velocity signal $\tilde{u}(t)$ in comparison with edge displacement signal $\eta(t)$ and resultant phase difference $(\phi_{\tilde{u}}-\phi_\eta)$ at frequency ratio $f_e/f_0^* = 0.87$.

displacement $\eta(t)$ and the bottom plot represents the instantaneous phase difference $(\phi_{\tilde{u}}-\phi_\eta)$ between the phase $\phi_{\tilde{u}}$ of the velocity fluctuation $\tilde{u}$ and the phase ϕ_η of the edge at its maximum positive displacement. This phase difference is also represented by the bold horizontal bars indicating the distance between the peaks of the edge displacement $\eta(t)$ and the velocity fluctuation $\tilde{u}(t)$. This type of characterization of the near-wake velocity fluctuations, as well as the surface pressure fluctuations, was carried out for ranges of f_e/f_0^* above, and below, $f_e/f_0^* = 1$ (Lotfy 1988). In general, the modulations of the pressure traces were found to parallel closely those of the instantaneous velocity

traces, as described by Lotfy (1988). On the basis of the similarity of the time-dependent surface pressure on the surface of the trailing edge and the velocity fluctuations downstream of the edge, one may conclude that the highly ordered process of modulation occurs throughout the near-wake region. It is a global phenomenon and not simply limited to a localized region of the edge, or to a given downstream location of the flow. The existence of these quasi-periodic regimes is in general accord with the numerical simulations of Karniadakis & Triantafyllou (1989*a*). In fact, the general form and the period of the modulation are in accord, at least for $f_e/f_0^* = 1$, with their calculations.

The variation of the phase difference $(\phi_{\tilde{u}} - \phi_{\mu})$ shown in figure 3 is representative of the variations obtained in the range of excitation $f_e/f_0^* < 0.95$; $(\phi_{\tilde{u}} - \phi_{\eta})$ decreases for successive cycles of the edge oscillation, with phase jumps occurring at the end of each oscillation cycle. Defining N as the number of cycles of edge oscillation that make up a complete modulation cycle, the value of N increases as the frequency ratio f_e/f_0^* increases. The converse holds for excitation over the range $f_e/f_0^* > 1.05$. The length of the modulation cycle, and thereby the value of N, is repeatable over a number of cycles of the edge oscillation (Lotfy 1988).

Moreover, the slope of the line connecting the dots in the plots of $\phi_{\tilde{u}} - \phi_{\eta}$ *vs.* t is equal to the difference between the inherent vortex formation frequency f_0 and the forcing frequency f_e. Mathematically, this relationship can be expressed as

$$\mathrm{d}\phi/\mathrm{d}t = \mathrm{d}(\phi_{\tilde{u}} - \phi_{\eta})/\mathrm{d}t = f_0 - f_e \quad \text{or} \quad f_e - f_0$$

the first being valid for $f_e/f_0^* < 0.95$ and the second for $f_e/f_0^* > 1.05$. Analogous relations hold for the phase $\phi_{\tilde{p}}$ of the pressure relative to the phase ϕ_{η} of the edge displacement, i.e. $\phi_{\tilde{p}} - \phi_{\eta}$.

The foregoing observations indicate the trace existence of modulation phenomena in the vortex shedding process. In this case, f_0 may be viewed as the carrier frequency and $f_m = f_0 - f_e$ as the modulation frequency for $f_e/f_0^* < 0.95$; for $f_e/f_0^* > 1.05$, f_e would be the carrier frequency and $f_m = f_e - f_0$ the modulation frequency. In the following, we characterize these modulation processes.

4.2. *Classes of modulation of the near wake and time-averaged spectra of velocity and pressure*

Excitation of the wake over the range of dimensionless frequency $0.5 \leqslant f_e/f_0^* \leqslant 2.0$ revealed that several types of modulation can occur, based on inspection of the instantaneous time traces and the spectral content of the velocity and pressure signals.

Let χ represent either the instantaneous velocity or pressure. For pure amplitude modulation (AM),

$$\chi(t) = A_0[1 + m \sin \omega_m t] \cos \omega_0 t, \tag{1}$$

in which $0 < m \leqslant 1$. For phase modulation (PM),

$$\chi(t) = A_0 \cos [\omega_0 t + m \sin \omega_m t], \tag{2}$$

and for frequency modulation (FM),

$$\chi(t) = A_0 \cos [\omega_0 t + (\Delta\omega/\omega_m) \sin \omega_m t], \tag{3}$$

in which $\Delta\omega$ is the maximum frequency deviation. Comparing equations (2) and (3), we see that the modulation index m for FM varies inversely with modulation frequency ω_m, while for PM it is independent of frequency. Generally speaking, FM is the general form of PM.

In this study, the definition of the 'carrier' frequency varies according to the value of f_e/f_0^*. When $f_e/f_0^* < 1$, the carrier frequency is the natural shedding frequency

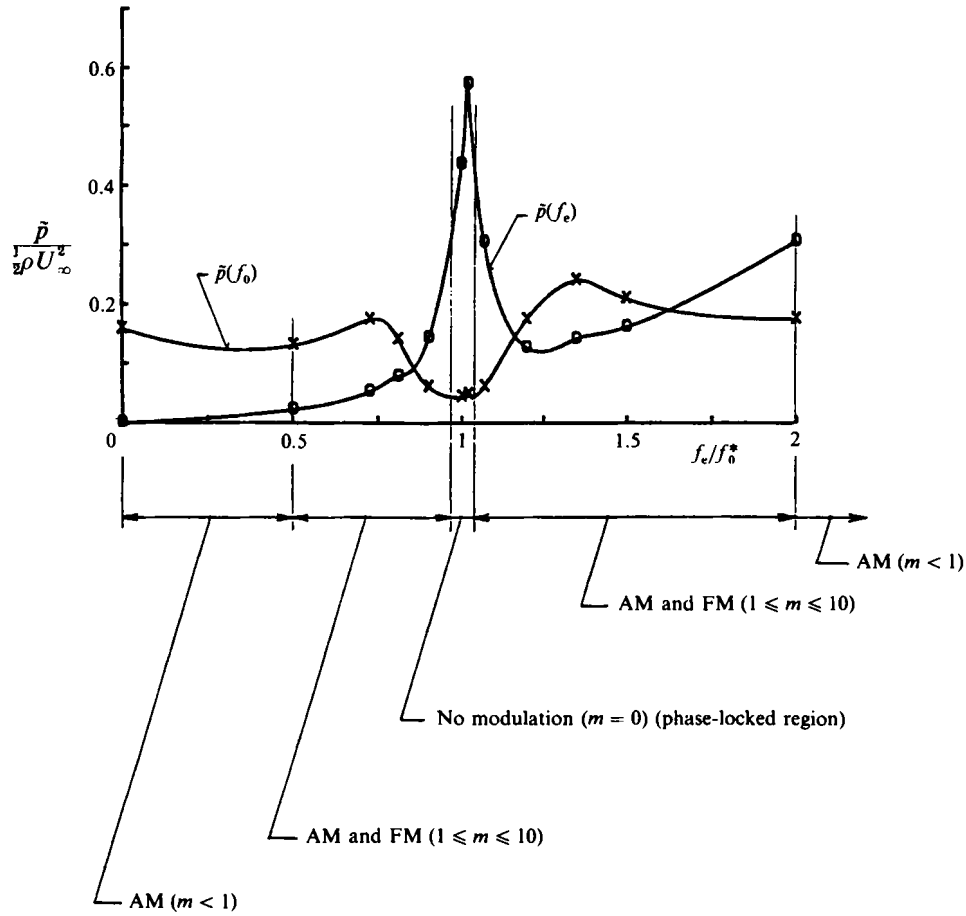

FIGURE 4. Types of modulation at different f_e/f_0^* as function of m for surface pressure fluctuation $\tilde{p}$. Parameter m is a modulation index, equal to the number of edge oscillation cycles required for one vortex modulation cycle.

component $\omega_0 = 2\pi f_0$ because $f_0 > f_e$, while for $f_e/f_0^* > 1$, the carrier frequency is the forced frequency component $\omega_e = 2\pi f_e$ because $f_e > f_0$.

For $f_e/f_0^* < 1$: $\omega_m = \omega_0 - \omega_e$ and $\Delta\omega = \omega_0 - \omega_m = \omega_e$. Then $m = \Delta\omega/\omega_m = \omega_e/[\omega_0 - \omega_e] = N$.

For $f_e/f_0^* > 1$: $\omega_m = \omega_e - \omega_0$ and $\Delta\omega = \omega_e - \omega_m = \omega_0$. Then $m = \Delta\omega/\omega_m = \omega_0/[\omega_e - \omega_0] = N$.

An important observation is that the number of edge oscillations N needed to make up a modulation cycle of the vortex shedding process is frequency dependent. It can be expressed in terms of the modulation index m, which varies inversely with the modulation frequency $\omega_m = 2\pi f_m$.

On the basis of considering $\chi(t)$, i.e. instantaneous velocity or pressure signals, in conjunction with their spectral content, it is possible to define the classes of modulation which can occur over the wide range of excitation frequency f_e/f_0^* (Lotfy 1988). Figure 4 shows a typical response curve $\tilde{p}/\frac{1}{2}\rho U_\infty^2$ *vs.* f_e/f_0^*, in which $\tilde{p}$ is the time-averaged amplitude of the pressure fluctuation. Symbols $\tilde{p}(f_0)$ and $\tilde{p}(f_e)$ correspond to the spectral peaks at f_0 and f_e. No modulation occurs in the phase-locked region, i.e. in the immediate vicinity of $f_e/f_0^* = 1$. Otherwise, there are combinations of AM and FM, or AM alone, if the value of f_e/f_0^* is sufficiently high or low. The important point to be

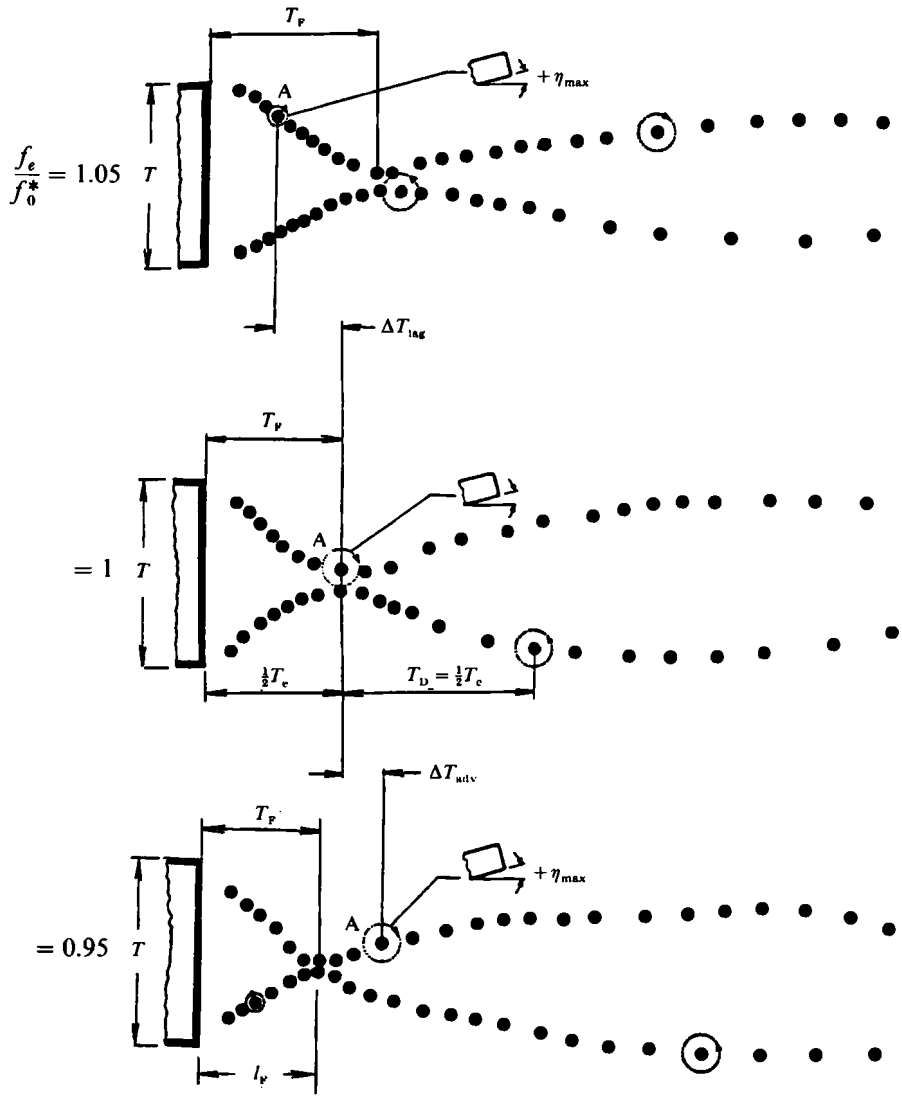

FIGURE 5. Timescales for vortex shedding process from oscillating edge in phase-locked region of excitation ($f_e/f_0^* = 0.95$, 1, 1.05).

emphasized here is that time-averaged amplitudes of pressure, lift, or velocity, which have been measured in a wide range of investigations, may be the consequence of complex processes of modulation and not reflect the actual physics of the near wake.

5. The phase-locked wave: vortex trajectories

Attention is now devoted exclusively to the phase-locked region of the near-wake response, confined to the region $0.95 \leqslant f_e/f_0^* \leqslant 1.0$, and illustrated by the flow visualization of figure 1. As evident therein, there are large changes in the timing of the initially formed vortex for small changes in excitation frequency f_e/f_0^*.

Since the vortex formation process is phase locked with respect to the edge motion, it is desirable to track the trajectories of the vortices in order to relate the instantaneous location of a tyical vortex relative to the instantaneous position of the edge. Figure 5 shows the trajectories of vortices shed from the upper and lower corners of the trailing

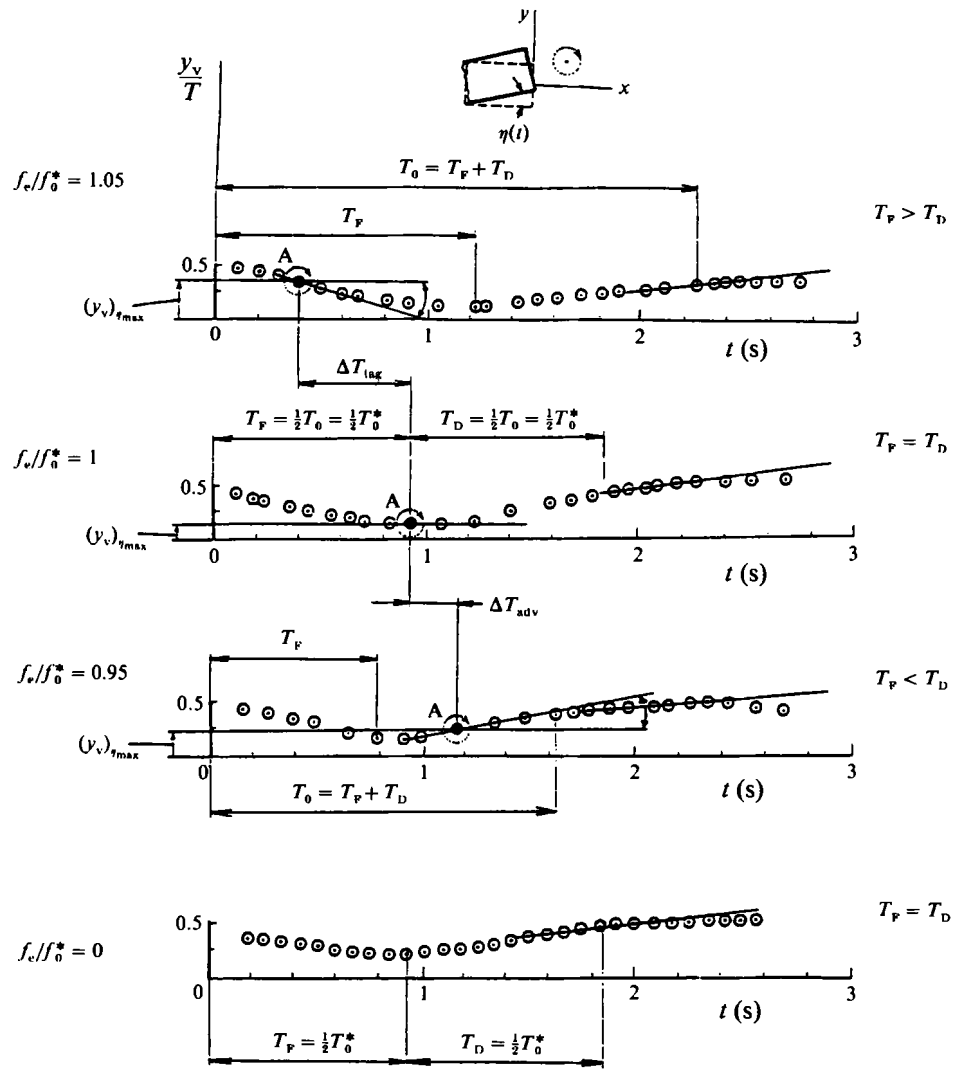

FIGURE 6. Timescales for vortex shedding process from stationary edge ($f_e/f_0^* = 0$) and from oscillating edge in the phase-locked region of excitation ($f_e/f_0^* = 0.95$, 1, 1.05).

edge; the successive instantaneous positions of a given vortex are indicated by the black dots. The time between the black dots is constant for all cases.

The dotted circles surrounding selected black dots represent the instantaneous positions of the vortices when the edge is at its maximum positive location, i.e. $+\eta_{max}$. If one designates a reference vortex by A, it is evident that the location of this vortex A moves towards the trailing edge with increasing f_e/f_0^*. Likewise, the vortex on the lower side of the near-wake vortex street moves towards the edge as well.

After the vortex reaches its location closest to the centreline of the flow, there is an abrupt increase in velocity as it 'departs' and moves outward away from the centreline. The vortex formation length l_F is defined to occur when the position of the vortex is closest to the centreline of the flow; it requires a time T_F. As illustrated in figure 5, an increase in f_e/f_0^* produces an increase in l_F. Visualization showed that, irrespective of the value of f_e/f_0^*, there is abrupt termination of the ingestion of boundary-layer fluid (i.e. vorticity-bearing fluid from the corner of the edge) into the vortex when it is

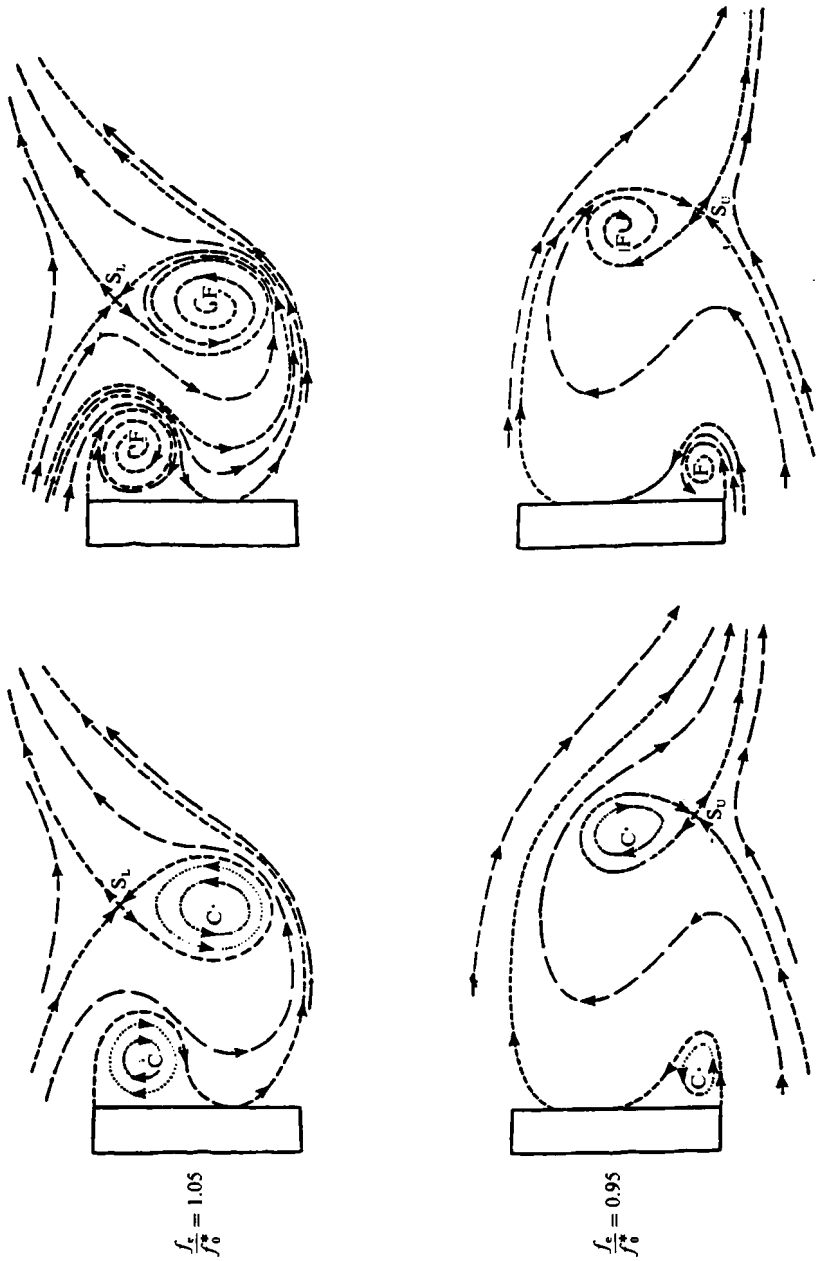

FIGURE 7. Possible topological representation of near wake assuming two-dimensional structure (left column) and three-dimensional structure (right column).

closest to the centreline of the wake. In other words, when the vortex is at the position l_F, the vortex formation process is completed, in that the boundary-layer fluid ceases to be drawn into the vortex. Remarkable is the fact that this definition holds irrespective of the phase shift between the vortex formation process and the instantaneous position of the edge.

For the special case of 'synchronized' oscillations of the edge at $f_e/f_0^* = 1$, the upper vortex is at the position l_F when the edge is at its maximum positive position. This means that the upper vortex forms while the edge moves from its maximum negative position $-\eta_{max}$ to its maximum positive position η_{max}, and conversely for the lower vortex. On the other hand, at $f_e/f_0^* = 0.95$, the formation of the upper vortex leads the motion of the edge, while at $f_e/f_0^* = 1.05$, it lags the motion of the edge.

The trajectories of figure 5 can be plotted in the form of streamwise and cross-stream displacements x_v and y_v of the vortex *vs.* time t (Lotfy 1988), as illustrated in figure 6. Here we consider the trajectories y_v/T shown in figure 6. These trajectories at $f_e/f_0^* =$ 0.95, 1.0, 1.05 are compared with those for the stationary trailing edge at $f_e/f_0^* = 0$. For all trajectories corresponding to the oscillating trailing edge, the location of the vortex at the instant when the trailing edge is at its maximum positive position η_{max} is indicated by the circle A. At this instant, the vortex is located at $(x_v)_{\eta_{max}}$.

The vertical velocity dy_v/dt of the vortex, when the edge is at its maximum positive position $+\eta_{max}$, is indicated schematically by the slopes of the y_v *vs.* t trajectories at the location A in figure 6. These slopes show that, at $f_e/f_0^* = 1$, the vertical velocity is zero, while at $f_e/f_0^* = 0.95$ and 1.05, it has substantial positive and negative values respectively.

It is possible to relate the trajectories shown in figure 6 to the period T_0 of the vortex shedding process, which can be determined precisely from pressure or velocity measurements (Lotfy 1988). The period T_0 is defined as the sum of the vortex formation time T_F and the vortex departure time T_D, i.e. $T_0 = T_F + T_D$. According to the definition of the vortex formation length l_F given in figure 5, the formation time T_F is the time elapsed until the vortex reaches its maximum negative position (position closest to the centreline of the flow). The departure time T_D is then the difference between the times T_0 and T_F. (The physical justification for defining T_F and T_0 is given in §6.2.1.) Figure 6 shows these timescales for the values of excitation frequency $f_e/f_0^* = 0$, 0.95, 1 and 1.05. For the case $f_e/f_0^* = 1$, $T_e = T_0 = T_0^*$, in which T_0^* is the period of the vortex shedding process from the stationary edge and T_e is the period of the edge motion. Moreover, the vortex formation time T_F is equal to the vortex departure time T_D, i.e. $T_F = T_D$. For values of excitation frequency $f_e/f_0^* = 0.95$ and $f_e/f_0^* = 1.05$, the values of T_F are respectively smaller and larger than that at synchronization.

As depicted in the overview of figure 5, these differences in formation time T_F are the source of the phase shifts, or the advance and lag times, between the vortex formation and the edge motion. In the case $f_e/f_0^* = 0.95$, the vortex formation leads the edge motion by an advance time ΔT_{adv}, while in the case $f_e/f_0^* = 1.05$, the vortex formation lags the edge motion by a lag time ΔT_{lag}.

The magnitudes of these advance and lag times will be related to the physics of the vortex formation and departure processes in the next section.

6. Phase-locked wake: topological structure and phase clock representation

In order to provide a basis for describing the changes in the near-wake flow structure as a function of excitation conditions of the trailing edge, it is desirable to employ basic

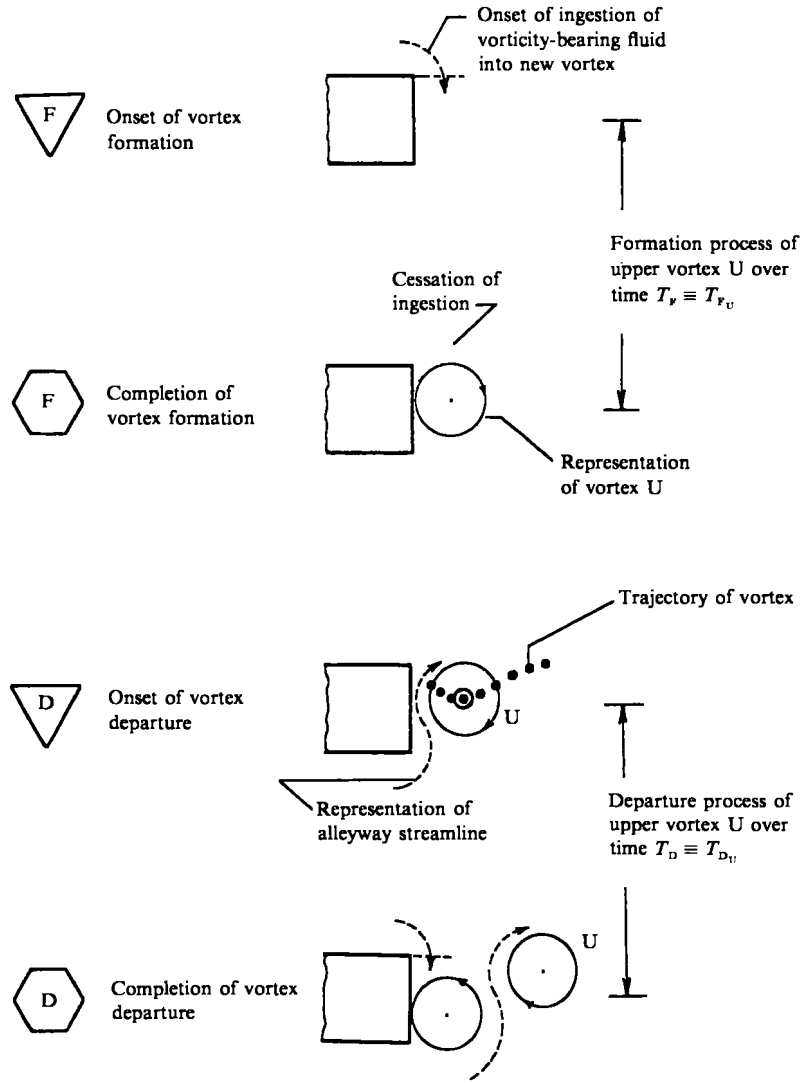

FIGURE 8. Definition of terminology for phase clocks.

concepts of flow topology. Detailed descriptions and assessments of topological concepts applied to various unsteady, separated flows are given in the series of investigations of Perry and his colleagues, the most recent and directly relevant of which addresses vortex formation in the near wake (Steiner & Perry 1987). In the following, details of topological patterns are given for selected cases. Then, simplified representations of these patterns are given over a complete cycle of oscillation of the trailing edge, allowing interpretation of the mechanisms that give rise to the phase shift between the vortex formation process and the edge motion.

6.1. *Representative topological structure*

The topological flow pattern generated from the oscillating trailing edge depends upon the frequency ratio f_e/f_0^* and the instantaneous position of the edge during an oscillation cycle. It is, therefore, desirable to select the most physically significant values of f_e/f_0^* and examine the topology at the same instantaneous position (i.e. phase) of the edge in order to obtain a direct cross-comparison of the flow structure.

Excitation at the frequency ratios $f_e/f_0^* = 0.95$ and 1.05 generates the representative types of wake structure within the phase-locked range (see figure 1). The wake structure at these two values of f_e/f_0^* is approximately π out-of-phase at the same instantaneous position of the edge.

In order to determine the instantaneous velocity field, small hydrogen bubble elements were tracked in conjunction with a frame-by-frame analysis of the videotape. Details, as well as the raw velocity fields, are given by Lotfy (1988). Representations of the near-wake topology based on these data are given in figure 7. At each frequency ratio f_e/f_0^*, the flow structure is shown at the same instantaneous position of the edge corresponding to $\theta_e = -20°$ before reaching the maximum positive position $+\eta_{max}$ of the edge, i.e. prior to attainment of top dead centre of the edge motion ($\theta_e = 0°$). (A complete oscillation cycle is defined to occur over $\Delta\theta_e = 360°$.)

The two admissible interpretations of these streamline patterns are given in the left and right columns of figure 7. The symbols indicate the key topological features defined as follows: S = saddle point of completely formed vortex; F = focus of vortex; C = centre of vortex; $(\,)_U$ = parameter of vortex formed from upper corner of edge; $(\,)_L$ = parameter of vortex formed from lower corner of edge.

For the frequency ratio $f_e/f_0^* = 0.95$ shown in figure 7, the lower vortex, adjacent to the corner of the edge, is in the process of formation; it involves the ingestion of vorticity-bearing fluid from the separating boundary layer. On the other hand, the upper vortex, located further downstream of the edge, is departing from the near-wake region. This departure is aided by the alleyway flow, corresponding to irrotational fluid drawn from the lower side of the wake, and up around the vortex in the clockwise direction. The corresponding foci and centres of the three- and two-dimensional representations of the vortices are indicate as F and C. For both representations of the flow structure, there is a saddle point S on the lower side of the vortex originally formed from the upper side of the trailing-edge.

At the frequency ratio $f_e/f_0^* = 1.05$, there is a phase shift of approximately π of the topological map, relative to that for $f_e/f_0^* = 0.95$. The lower vortex is departing the near-wake region while the upper vortex is still in its formation process, defined by ingestion of vorticity-bearing fluid from the separated boundary layer.

6.2. *Simplified representation of topological flow structure via phase clocks*

From the foregoing flow visualization (figure 1) and representative topology (figure 7), it is evident that f_e/f_0^* can have a profound effect on the structure of the near wake. A complete description of the changes requires consideration of not only the values of f_e/f_0^*, but also the variation of the topological structure during the oscillation cycle of the trailing edge. Simplified representations of the near-wake topology are defined in the following. These representations are then employed to represent the variation of the wake structure over an entire oscillation cycle by means of a phase clock concept.

6.2.1. *Definitions and concepts of phase clock*

Before proceeding with the actual description of the near wake, it is necessary to define the abbreviated sketches and symbols given in figure 8. In essence, for a given vortex, there are two basic processes that occur: formation of the vortex; and departure of the vortex from the near-wake region. In order to define precisely the time T_F elapsed during vortex formation and the time T_D elapsed during departure of a vortex, it is desirable to employ the terminology given in figure 8. Onset of vortex formation is taken to occur when there is onset of ingestion of vorticity-bearing fluid past the corner of the edge; in other words, when the separating boundary layer is

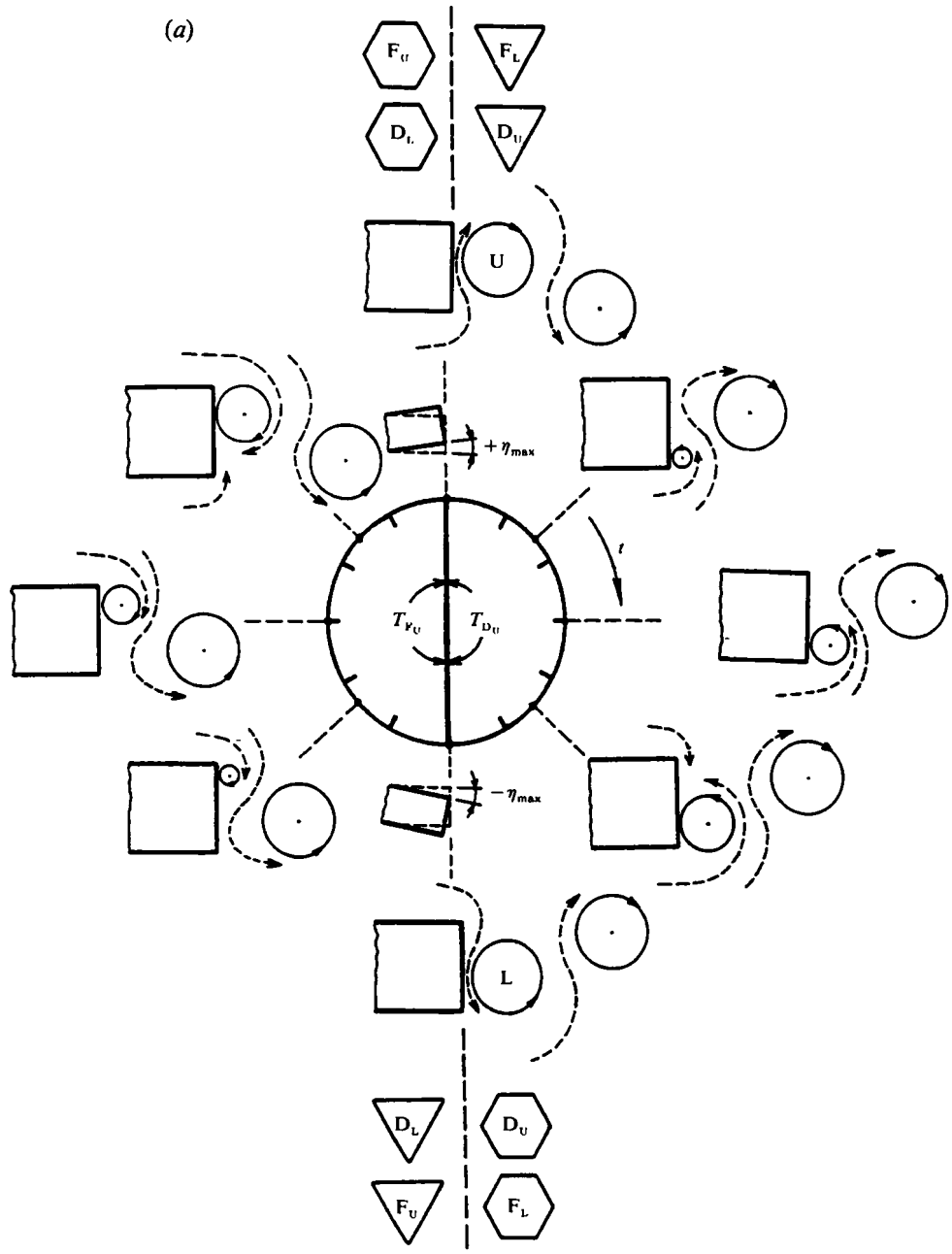

FIGURE 9(*a*). For caption see p. 191.

swept past the corner, the vortex formation begins. Completion of vortex formation occurs when there is no longer ingestion of vorticity-bearing fluid past the corner of the edge. The onset of vortex formation is represented by the symbol F within a triangular 'yield' sign, and completion of vortex formation by the symbol F within a hexagonal 'stop' sign.

Onset of vortex departure is defined to occur when the focus or centre of the vortex reaches its location closest to the centreline of the wake indicated schematically in figure 8. (Recall, as shown in figures 5 and 6, that the trajectory of a typical vortex first

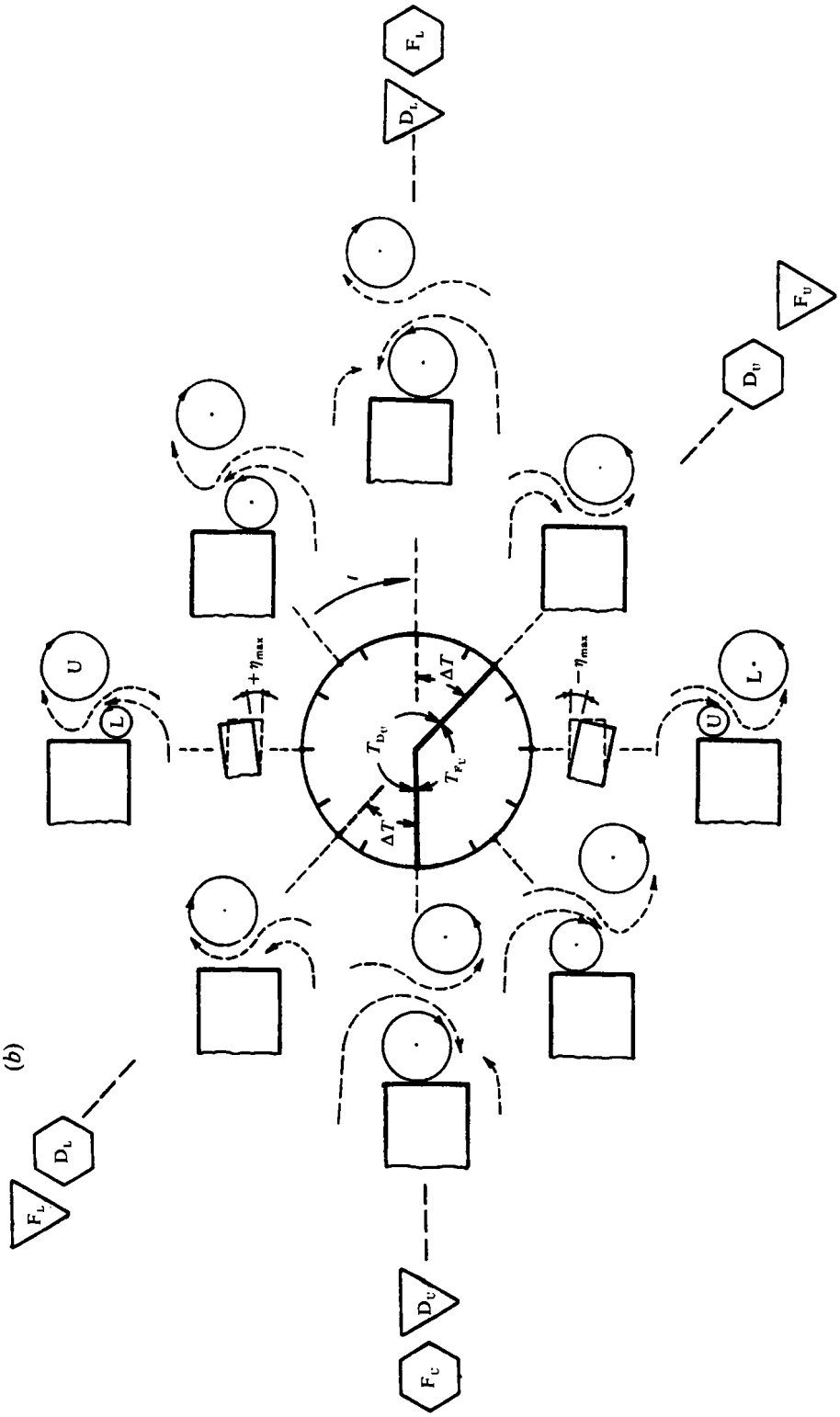

FIGURE 9(*b*). For caption see facing page.

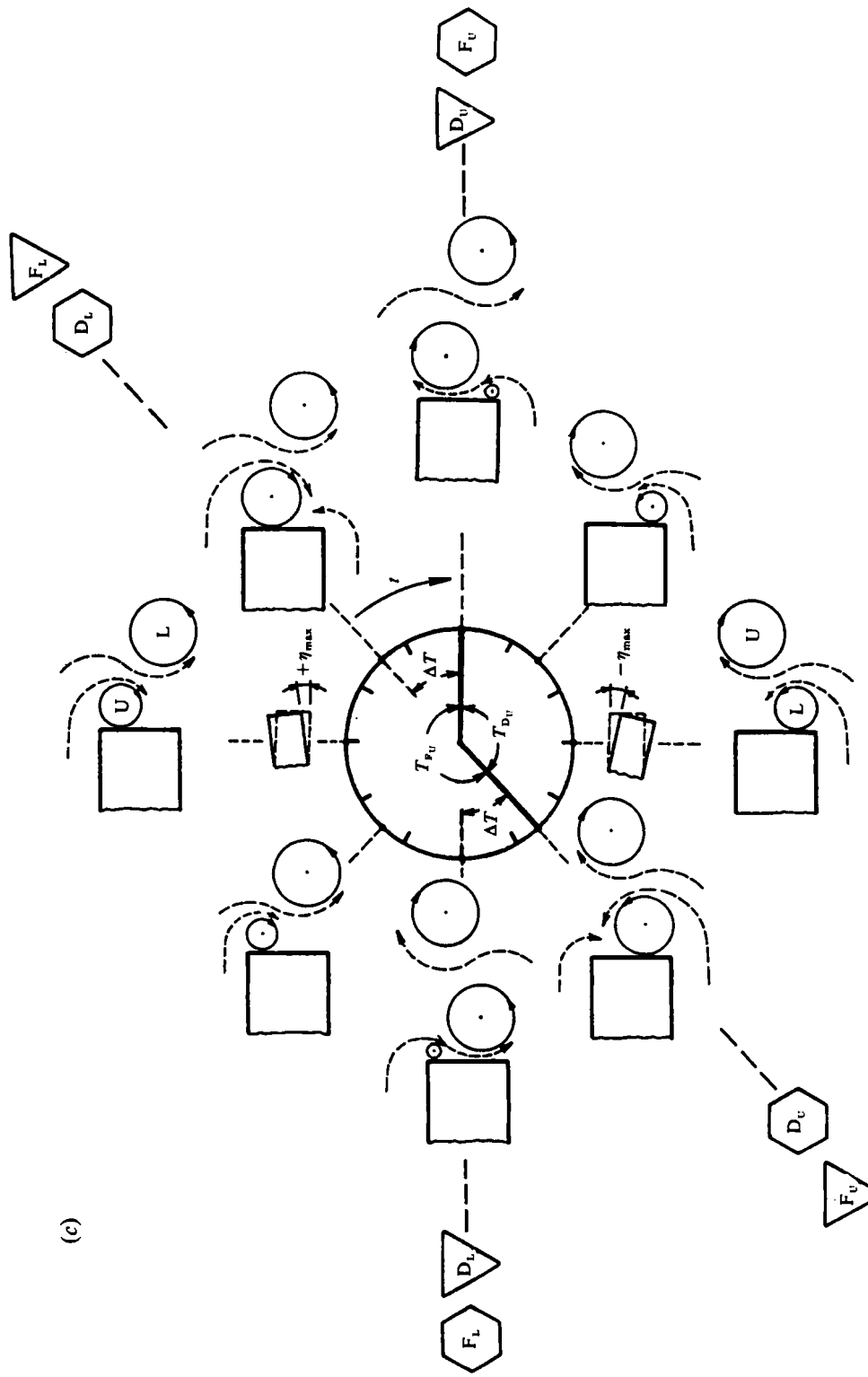

FIGURE 9. Phase clock representation of vortex shedding process at (*a*) $f_e/f_0^* = 1$, (*b*) $f_e/f_0^* = 0.95$, (*c*) $f_e/f_0^* = 1.05$.

moves towards the centreline of the near wake, then away from it.) At, or immediately after, the onset of departure of the vortex, fluid drawn from the opposite side of the wake is represented by the alleyway streamline extending across the entire wake. This alleyway streamline is located between the vortex and the trailing edge as indicated in figure 8. The process of vortex departure is completed when the onset of formation of a new upper U vortex begins. As shown schematically in figure 8, the onset of departure is indicated by the symbol D within a triangular sign and its completion by the symbol D within a hexagonal sign.

Extensive study of the processes of vortex formation and departure reveals the following guidelines. For the special cases of the stationary trailing edge $f_e/f_0^* = 0$ and the edge oscillating at a frequency synchronized with the natural vortex shedding frequency $f_e/f_0^* = 1$, the completion of vortex formation on one side of the wake corresponds to onset of vortex formation on the other side of the wake. Likewise, completion of vortex departure on one side corresponds to onset of vortex departure on the other side. However, for all other excitation conditions $f_e/f_0^* \neq 1$ in the phase-locked region, there is a time shift ΔT between completion of formation of the vortex on, for example, the upper side of the wake and onset of formation of the next vortex on the lower side of the wake. Similarly, there is a time shift ΔT between completion of departure of the upper vortex and onset of departure of the lower vortex. The physical interpretation of this time shift ΔT will be explained subsequently.

Irrespective of the time shift ΔT, however, completion of formation of the upper U vortex corresponds to: the onset of its departure; and the onset of formation of its successor on the upper side. This means that the relation $T_{F_U} + T_{D_U} = T_e$ is always satisfied for the upper U vortex. Likewise, for the lower L vortex, $T_{F_L} + T_{D_L} = T_e$.

6.2.2. *Phase clock of near-wake at synchronization*

In order to illustrate the near-wake structure as a function of the excitation frequency of the edge, the concept of a phase clock is employed. The clock of figure 9(*a*) shows simplified representations of the instantaneous topological structure as a function of time t, which increases in the clockwise direction. The key features of the topological patterns are those associated with the onset and completion of the vortex formation and departure. Figure 9(*a*) schematically portrays these essential features using the symbols of figure 8. For the vortex formation F and departure D processes, subscripts U and L represent vortices formed from the upper and lower edges respectively. Therefore, the symbols F_U and D_U represent the formation and departure of a given vortex from the upper side of the edge. The triangular and hexagonal signs represent the beginning and end of vortex formation and departure respectively. At the centre of the phase clock, the vortex formation and departure times T_{F_U} and T_{D_U} for the upper U vortex are indicated. Similar terminology, though not illustrated, holds for the lower L vortex as well.

In figure 9(*a*), the maximum positive (upward) deflection of the trailing edge, indicated by $+\eta_{max}$, occurs at the 12:00 (twelve o'clock) location on the phase clock. Similarly, the maximum negative position of the edge η_{max} is at the 6:00 (six o'clock) location. As the edge reaches its maximum positive position, there is cessation of ingestion of vorticity-bearing fluid into the upper vortex, marking completion of the elapsed time T_{F_U} of formation and onset of departure of the vortex, which takes a total time T_{D_U}. Simultaneously, there is onset of formation of the lower vortex. When the edge reaches its maximum negative position, the roles of the upper and lower vortices are switched, and analogous events occur.

In summary, for vortex shedding from the edge oscillating at the synchronization

condition f_e/f_0^*, we have the remarkable result that all of the vortex formation and departure times have the same value and are equal to the half-period of $0.5T_0$ of vortex formation from the oscillating edge, which in turn is equal to the half-period $0.5T_0^*$ of vortex formation from the stationary edge, i.e. $0.5T_0 = 0.5T_0^* = T_{F_U} = T_{F_L} = T_{D_U} = T_{D_L}$.

6.2.3. *Phase clock of near-wake below synchronization*

Excitation at a frequency slightly below synchronization, represented by $f_e/f_0^* = 0.95$, produces the phase clock given in figure 9(*b*). For this excitation condition, the period T_0^* of the inherent vortex shedding from the stationary edge is less than the period T_e of the edge motion. In presence of the edge motion, however, T_0^* is modified to a value T_0. Quantitative measurement of T_0 shows that it satisfies the condition $T_0 < T_0^* < T_e$ as represented in figure 6. Since the condition $T_0 < T_e$ is satisfied, there will be a tendency for the processes of vortex formation and departure to occur at an earlier time on the phase clock. They will experience an advance in phase relative to that occurring for the synchronized case where $T_0 = T_0^* = T_e$, shown in figure 9(*a*). The onset of formation of the upper vortex, designated as F_U, occurs at 4:30 instead of at 6:00 for the synchronized case of figure 9(*a*). Likewise, the start of formation of the lower vortex designed as F_L occurs at 10:30 instead of 12:00 in the synchronized case.

Since the condition $T_0 < T_0^*$ is satisfied, the angles on the phase clock corresponding to elapsed times of formation T_F of the upper U and lower L vortices should be less than 180° (compare figure 9*a*). On the phase clock, the end of vortex formation is shifted in the counterclockwise direction. This shift, represented by ΔT, is from 10:30 to 9:00 in the case of the upper vortex designated as F_U (with a hexagonal 'stop' sign) and from 4:30 to 3:00 in the case of the lower vortex designated as F_L (with a hexagonal sign). This shift ΔT also represents, for example, the delay between the start of departure of the lower vortex at 3:00 indicated as D_L (with a triangular 'yield' sign) and the beginning of formation of the upper vortex at 4:30 indicated as F_U (with a triangular sign).

Physically interpreted, the time shift ΔT is associated with the processes of vortex formation and departure with respect to the edge motion. In the synchronized case, the upper vortex, for example, initiates formation when the edge starts its upper motion at 6:00 (compare figure 9*a*). However, for the case of figure 9(*b*), it initiates at 4:30 while the edge is still moving downward. In other words, the initial stage of formation of the upper vortex is contrary (or counter) to the direction of motion to the edge; the consequent retardation of this initial vortex formation contributes to the shift ΔT from completion of the formation of the lower vortex to the onset of formation of the upper vortex. This interval corresponds to the time between 3:00 and 4:30 on the phase clock. Moreover, during the same interval the direction of the edge motion is in accord with the circulation of the lower vortex, promoting early formation of the alleyway streamline extending across the near wake, in turn enhancing the early departure of the lower vortex. Analogous reasoning holds for the shift ΔT between 9:00 and 10:30 on the phase clock.

Generalizing, the time shift ΔT below synchronization ($f_e/f_0^* < 1$) is associated with the following influences: the downward motion of the edge is counter to that which promotes the initial formation of the vortex from the upper corner of the edge; this edge motion, however, matches the direction of the circulation of the vortex formed from the lower corner and matches the direction of the alleyway streamline that promotes departure of that vortex from the near-wake region. Similar reasoning holds for the upward motion of the edge.

Taking an overview of the phase clock of figure 9(*b*), we note that formation of the upper vortex F_U is completed at 9:00 (with hexagonal sign) instead of at 12:00 as occurs in the synchronization case (compare figure 9*a*). Likewise, the formation of the lower vortex F_L is completed at 3:00 (with a hexagonal sign) insteady of at 6:00 for the synchronization case (compare figure 9*a*). In other words, both of these processes are completed one-quarter cycle earlier than in the synchronized case. This shift corresponds to $0.25T_e$ on the phase clock. Keeping in mind that $T_0^* = 0.95T_e$, one may state that a deviation of $0.05T_e$ between the period T_e of the edge motion and the period T_0^* of the inherent vortex formation from the stationary edge produces a fivefold 'amplification' in the time of advancement of the completion of vortex formation and departure.

6.2.4. *Phase clock of near-wake above synchronization*

For excitation at a frequency f_e greater than the inherent shedding frequency f_0^* from the stationary edge, i.e. $f_e/f_0^* = 1.05$, quantitative measurements represented in figure 9(*c*) show the relation $T_0 > T_0^* > T_e$. Since $T_0 > T_e$, the vortex formation will tend to occur later during the oscillation cycle, i.e. it will be retarded in phase relative to the synchronization case at $f_e/f_0^* = 1$ shown in figure 9(*a*). As illustrated in figure 9(*c*), onset of vortex formation from the upper side F_U now occurs at 7:40 in comparison with 6:00 for the synchronized case (compare figure 9*a*). For the lower vortex, the onset of formation now occurs at 1:40 in comparison with 12:00 for the synchronized case.

Since $T_0 > T_0^*$, the angles on the phase clock corresponding to formation times T_F of the lower L and upper U vortices should be greater than 180° (compare figure 9*a*). This simply means that the end of vortex formation will be shifted in the clockwise direction. Figure 9(*c*) shows a time shift ΔT from 1:40 to 3:00 in the case of the upper vortex designated as F_U (with a hexagonal sign) and from 7:40 to 9:00 in the case of the lower vortex designated as F_L (with a hexagonal sign).

From a physical standpoint, in analogy with the mechanism of figure 9(*b*), the shift ΔT is associated with the vortex formation and departure processes with respect to the edge motion. For the upper vortex, for example, in its initial stage of formation (starting at 7:40) is accompanied by upward motion of the edge, enhancing the formation process of the upper vortex. On the other hand, it is simultaneously counter to the direction of circulation of the lower vortex and counter to the direction of the alleyway streamline that is associated with departure of the lower vortex. In summary, the time shift ΔT above synchronization ($f_e/f_0^* > 1$) is associated with the following effects: the upward motion of the edge is in the same direction as that which promotes formation of the vortex from the upper corner. On the other hand, the edge motion is opposite to the circulation of the lower vortex; it is also counter to the direction of the alleyway streamline that promotes the departure process of the vortex on the lower side of the wake. Analogous reasoning holds for the downward motion of the edge.

In analogy with the case of figure 9(*b*), we note that the time for completion of formation of the upper vortex U, indicated by F_U within a hexagonal sign, extends to 3:00 instead of to 12:00 as for the synchronization case of figure 9(*a*). Likewise, the time for completion of formation of the lower vortex designated by F_L within a hexagonal sign extends to 9:00 instead of 6:00 as for the synchronization case. In other words, both of these processes are completed one-quarter cycle later than in the synchronization case. This delay corresponds to a total time $0.25T_e$ on the phase clock. There clearly exists an amplification of a small difference between the inherent vortex shedding at T_0^* and the edge T_e, i.e. $T_0^* = 1.05T_e$; it produces a fivefold time shift in the aforementioned processes.

Taking together the advance in time ($0.25T_e$) of completion of vortex formation with respect to the edge motion for the case of $f_e/f_0^* = 0.95$ and the delay in time ($0.25T_e$) of completion of vortex formation with respect to the edge motion for the case of $f_e/f_0^* = 1.05$, there will be a total phase difference $\Delta\phi = 0.5T_e$, or in terms of radius, $\Delta\phi = \pi$. In fact, this phase difference approximates that found in lift and pressure measurements in the wide variety of investigations cited in the Introduction. It will be further addressed in §7.

7. Overview of modulation and phase-shift

In §§3–6, it was demonstrated that the modulated and phase-locked wakes involve phase shifts of the vortex shedding with respect to the edge motion. These types of phase shift can be related to the frequencies of: the edge motion (f_e); the vortex shedding from the stationary edge (f_0^*); and the shedding from the oscillating edge (f_0). In the following, we first address the case of the modulated wake, then the phase-locked wake.

7.1. *Modulation at excitation frequencies below synchronization*

When the edge oscillates below synchronization, i.e. in the region $f_e/f_0^* < 1$, $T_e > T_0^* > T_0$. The elapsed time for the edge to go from the maximum negative position $-\eta_{max}$ to the maximum positive position $+\eta_{max}$ is $0.5T_e$. The upper vortex completes its formation before the edge reaches its maximum positive position $+\eta_{max}$, i.e. the vortex formation process leads the edge motion, as shown in figures 5 and 6. Designate this time interval, between completion of formation of the upper vortex and the attainment of the maximum positive position $+\eta_{max}$ of the oscillating edge, as an advance time 0.5τ for one half-cycle of the edge oscillation. If the same advance time occurs for formation of the lower vortex, then the total advance time over one complete cycle of the edge oscillation is

$$\tau = T_e - T_0. \tag{4}$$

Now this same advance time will be evident in the corresponding traces of surface pressure or wake velocity, as represented in the simulations of figure 10(*a*). In fact, as illustrated therein, the effect of this advance time τ is an additive one from cycle to cycle. When the edge starts its second cycle by moving up again to the maximum positive position $+\eta_{max}$, the total advance time becomes 1.5τ; completion of the second oscillation cycle of the edge, marked by attainment of the maximum negative position $-\eta_{max}$, gives a total advance time 2τ, and so on. In general, the total advance time may be expressed as $N\tau$. When it becomes equal to the period T_0, a complete modulation cycle is attained. In summary,

$$N\tau = T_0, \tag{5}$$

in which N is the number of edge oscillation cycles corresponding to one modulation cycle.

The value of N can be determined as follows. Equation (4) may be written as

$$\tau = [T_e/T_0 - 1]\,T_0. \tag{6}$$

Combining (5) and (6) gives

$$N = T_0/T_e/[1 - T_0/T_e] = f_e/f_0/[1 - f_e/f_0]. \tag{7}$$

Alternatively, one may write the expression for N by considering the relation

$$T_0/T_e = [T_0^*/T_e]/[T_0^*/T_0], \tag{8}$$

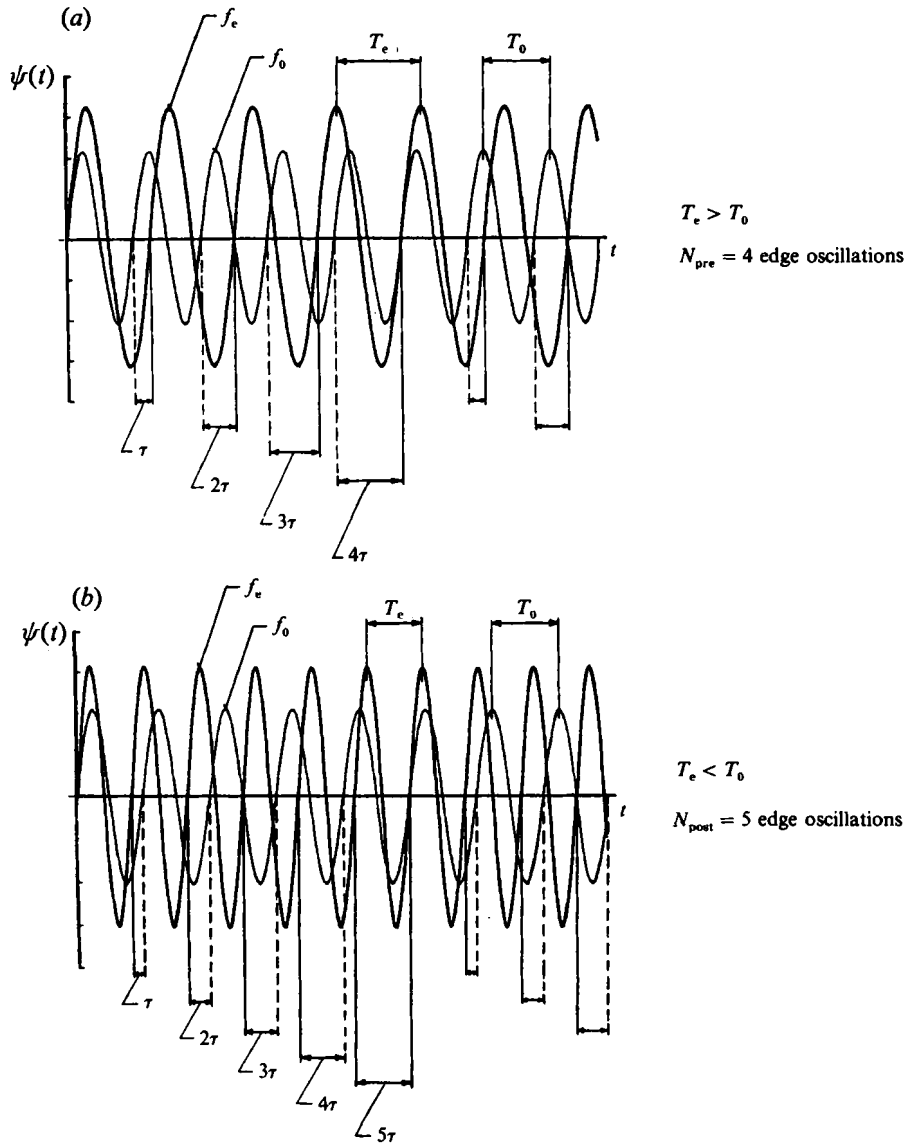

FIGURE 10. Simulated time traces of parameter $\psi(t)$, representing pressure or velocity, where τ is the advance time between T_e and T_0 in one oscillation: (*a*) for pre-synchronization condition $f_e/f_0^* < 1$; (*b*) for post-synchronization condition $f_e/f_0^* > 1$.

in which T_0^* is the corresponding period of vortex formation from the stationary edge. Combining (7) and (8):

$$N = T_0^*/T_e/[T_0^*/T_0 - T_0^*/T_e] = f_e/f_0^*/[f_0/f_0^* - f_e/f_0^*]. \tag{9}$$

This relation is plotted as the left branch of figure 11(*a*), using values of f_0/f_0^* determined from spectra of the near-wake velocity fluctuation.

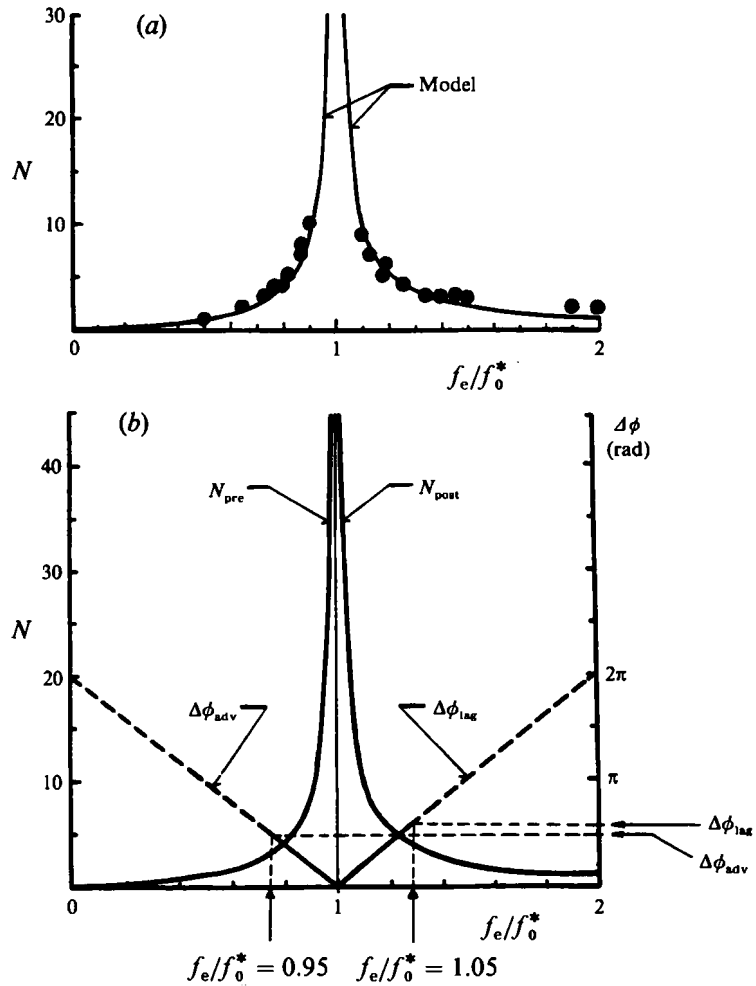

FIGURE 11. (*a*) Comparison between model and experimental values of the number N of edge oscillation cycles corresponding to one modulation. (*b*) Calculated results from theoretical model of modulation in near-wake region, where N is number of cycles of edge oscillation for one modulation cycle and $\Delta\phi$ is difference in phase of upper vortex at synchronization condition $f_e/f_0^* = 1$ and that at any other frequency ratio f_e/f_0^* in phase-locked region.

7.2. *Modulation at excitation frequencies above synchronization*

When the edge oscillates above synchronization, $T_e < T_0^* < T_0$. The upper vortex completes its formation after the edge passes its maximum positive position $+\eta_{max}$, i.e. the vortex formation process lags the edge motion, as shown in the schematics of figures 5 and 6.

Using analogous reasoning as for the pre-synchronization region described in §7.1, one obtains a lag time τ in the simulated traces of surface pressure and wake velocity, as represented in figure 10(*b*). The corresponding number of modulation cycles is

$$N = f_0/f_0^*/[f_e/f_0^* - f_0/f_0^*]. \tag{10}$$

This relation is plotted as the right branch of figure 11(*a*).

Experimental data for the values of N obtained from velocity and pressure measurements are shown on the left and right branches of figure 11(*a*); the agreement with the curves representing (9) and (10) is satisfactory.

7.3. *Phase variation within the phase-locked region*

Within the phase-locked region, the concept of a modulation cycle becomes irrelevant, and one may directly consider the equations for the advance and lag times above and below synchronization, which we designate as τ_{adv} and τ_{lag} respectively. They are defined by the advance-time equation (6) and its analogy for the lag time.

To transform the τ_{adv} and τ_{lag} to phase shifts $\Delta\phi_{adv}$ and $\Delta\phi_{lag}$, it is necessary to multiply by the circular frequency $2\pi f_e$, which corresponds to one cycle of edge oscillation. The resultant expressions are as follows:

$$\phi_{adv} = \tau_{adv}[2\pi f_e] = 2\pi(1 - f_e/f_0) = 2\pi(1 - [f_e/f_0^*]/[f_0/f_0^*]) \tag{11}$$

and

$$\phi_{lag} = \tau_{lag}[2\pi f_e] = 2\pi(f_e/f_0 - 1) = 2\pi([f_e/f_0^*]/[f_0/f_0^*] - 1). \tag{12}$$

These equations are plotted as dashed lines in figure 11(*b*). They are superposed on the plots of the parameter N. Subscripts pre and post designate regions below $f_e/f_0^* < 1$ and above $f_e/f_0^* > 1$, the synchronization condition. To calculate the total phase difference, we take the reference of the phase calculation to be the maximum positive position of the edge. It follows that

$$\begin{aligned}\Delta\phi_{diff} = \phi_{lag} - (-\phi_{adv}) &= \phi_{lag} + \phi_{adv} \\ &= 2\pi([f_e/f_0^*]/[f_0/f_0^*])_{post} - 2\pi([f_e/f_0^*]/[f_0/f_0^*])_{pre}.\end{aligned} \tag{13}$$

Equation (13) gives the phase difference of vortex shedding (with respect to the edge motion) between any values of frequency ratio in the pre-synchronization and post-synchronization ranges provided there is phase locking of the vortex shedding process with respect to the edge motion, i.e. if there is no modulation of the vortex shedding. As an approximation, it is valid when the modulation cycle contains a large number of edge oscillations very near the synchronization condition.

To calculate the phase difference from (13), it is necessary to know the values of the natural shedding frequency f_0. From the pressure or velocity measurements (Lotfy 1988) and using $f_e/f_0^* = 0.95$ and 1.05 for pre- and post-synchronization values, one obtains $f_0/f_0^* = 1.25$ and 0.85 respectively, and the phase difference from (13) is $\Delta\phi_{diff} = 0.95\pi$.

The values of $\Delta\phi_{lag}$, $\Delta\phi_{adv}$, and $\Delta\phi_{diff}$ are illustrated in figure 11(*b*). The value $\phi_{diff} = 0.95\pi$ does indeed represent well the phase difference given by the flow visualization of figure 1, as well as that determined from pressure and velocity measurements (Lotfy 1988).

8. Overview and conclusions

The wake from a stationary, blunt trailing-edge can exhibit a highly organized, self-excited oscillation. This oscillation has its origin in the linearly unstable near wake, described by the concepts of global (absolute) instability (Huerre & Monkewitz 1990). This self-excited instability of the wake is very robust and tends to persist even in the presence of oscillations of the trailing edge. In general, there are two predominant components existing in the near wake: that due to the self-excited wake instability and that imparted by the edge motion. The relative values of these frequency components determine whether the wake responds in a phase-locked or a modulated manner. The phase-locked response is, in fact, a limiting case of the modulated response. It is therefore insightful to gain an understanding of the characteristics of the modulated wake and use these concepts as a basis for describing the phase-locked wake.

The *modulated response* of the near wake is characterized by ordered and repetitive modulations of the flow structure. During a typical modulation cycle, the phase-referenced vortex pattern can drift in the streamwise direction by as much as $2.5T$, where T is the thickness of the trailing edge, even though the edge perturbation has a very small amplitude of the order of $0.05T$. These ordered and repetitive excursions of the near-wake vortices have their origin in the fact that the process of vortex formation from the oscillating trailing edge tends to lead (for dimensionless excitation frequency $f_e/f_0^* < 1$) or lag ($f_e/f_0^* > 1$) the motion of the edge. The total lag or lead is that accumulated over N cycles of the edge motion; the occurrence of N cycles of edge represents the period of the modulation cycle.

The surface pressure fluctuations on the edge and the velocity fluctuations in the near wake show this modulation of the near-wake flow structure, emphasizing the fact that it is a global phenomenon. From a practical standpoint, time-averaged measurements of pressure and lift on the surface of an oscillating body obscure pronounced amplitude/frequency modulations. Attempts to simulate or predict the loading on the surface of the edge should not assume that the flow structure of the near wake is periodic.

The *phase-locked response* of the wake occurs only near $f_e/f_0^* = 1$, i.e. when the edge excitation frequency is nearly matched to the natural vortex shedding frequency from the stationary edge. When the dimensionless excitation frequency f_e/f_0^* is varied by a small amount within this phase-locked range, there are large changes in the phase angle between the initially formed vortex and the position of the edge. If one views the phase-locked wake as a limiting case of the modulated wake, simple reasoning shows that the phase angle changes by approximately π when the dimensionless excitation frequency f_e/f_0^* of the edge changes between values corresponding to the upper and lower limits of the phase-locked region. This approach provides a basis for understanding the well-known phase jump of π observed in the large number of investigations that have measured either the phase angle of the fluctuating lift or the fluctuating surface pressure. An understanding of the mechanisms that produce this phase shift is essential, since it corresponds to a change in sign of the energy transfer between the fluid and the body.

The detailed flow structure of the phase-locked near wake has been interpreted in terms of simplified topological concepts. This approach, in conjunction with flow visualization, has allowed construction of a 'phase clock' that portrays the instantaneous phase of the edge motion at which vortex formation begins and ends as well as when vortex departure (from the near-wake region) begins and ends. These phase clocks are based on the concept that the total period of the vortex shedding is equal to the sum of the elapsed times for vortex formation from the edge and for vortex departure from the near-wake region.

The authors are grateful to the Office of Naval Research and the National Science Foundation for financial support of this investigation.

REFERENCES

BEARMAN, P. W. 1965 Investigation of the flow behind a two-dimensional model with a blunt trailing-edge and fitted with splitter plates. *J. Fluid Mech.* **21**, 241–255.

BEARMAN, P. W. 1984 Vortex shedding from oscillating bluff bodies. *Ann. Rev. Fluid Mech.* **16**, 195–222.

BERGER, E. & WILLE, R. 1972 Periodic flow phenomena. *Ann. Rev. Fluid Mech.* **24**, 313–340.

BLAKE, W. K. 1984 Trailing edge flow and aerodynamic sound. Part I: Tonal pressure and velocity fluctuations; Part II: Random pressure and velocity fluctuations. *Ship Acoustics Department, Research and Development Rep.* David W. Taylor Naval Ship, Research and Development Center, Bethesda, Maryland 20084-5000.

CHOMAZ, J. M., HUERRE, P. & REDEKOPP, L. T. 1988 Bifurcations to local and global modes in spatially developing flows. *Phys. Rev. Lett.* **60**, 25–28.

GERRARD, J. H. 1978 The wakes of cylindrical bluff bodies at low Reynolds number. *Phil. Trans. R. Soc. Lond.* A **288**, 351–389.

GRAHAM, J. M. R. & MAULL, D. J. 1971 The effects of an oscillating flap and an acoustic resonance on vortex shedding. *J. Sound Vib.* **18**, 371–380.

GREENWAY, M. E. & WOOD, C. J. 1973 The effect of beveled trailing-edge on cylinders. *J. Fluid Mech.* **61**, 323–335.

GRIFFIN, O. M. & RAMBERG, S. E. 1974 The vortex-street wakes of vibrating cylinders. *J. Fluid Mech.* **66**, 553–576.

HUERRE, P. & MONKEWITZ, P. A. 1990 Local and global instabilities in spatially developing flows. *Ann. Rev. Fluid Mech.* **22**, 473–538.

KOCH, W. 1985 Local instability characteristics and frequency determination of self-excited wake flows. *J. Sound Vib.* **99**, 53–83.

KARNIADAKIS, G. E. & TRIANTAFYLLOU, G. S. 1989*a* Frequency selection and asymptotic states in laminar wake. *J. Fluid Mech.* **199**, 441–469.

KARNIADAKIS, G. E. & TRIANTAFYLLOU, G. S. 1989*b* The crisis of transport measures in chaotic flow past a cylinder. *Phys. Fluids* A **1**, 628–630.

LOTFY, A. H. 1988 Flow structure and loading due to instabilities from an oscillating-edge of finite thickness. PhD dissertation, Department of Mechanical Engineering and Mechanics, Lehigh University.

LUSSEYRAN, D. & ROCKWELL, D. 1988 Estimation of velocity eigenfunction and vorticity distributions from the timeline visualization technique. *Expts Fluids* **6**, 228–236.

MONKEWITZ, P. A. 1988 The absolute and convective nature of instability in two-dimensional wakes as Reynolds numbers. *Phys. Fluids* **32**, 999–1006.

MONKEWITZ, P. A. & NGUYEN, L. N. 1987 Absolute instability in the near-wake of two-dimensional bluff bodies. *J. Fluids Struct.* **1**, 165–187.

MORKOVIN, M. 1964 Flow around circular cylinders – a kaleidoscope of challenging fluid phenomenon. *ASME Symp. on Fully Separated Flows*, pp. 102–118.

NAUDASCHER, E. & ROCKWELL, D. (ED.) 1980 *Practical Experiences with Flow-Induced Vibrations. Springer.*

OLINGER, D. J. & SREENIVASAN, K. R. 1988 Nonlinear dynamics of the wake of an oscillating cylinder. *Phys. Rev. Lett.* **60**, 797–800.

ONGOREN, A. & ROCKWELL, D. 1988*a* Flow structure from an oscillating cylinder. Part 1. Mechanisms of phase shift and recovery of the near-wake. *J. Fluid Mech.* **191**, 197–223.

ONGOREN, A. & ROCKWELL, D. 1988*b* Flow structure from an oscillating cylinder. Part 2. Mode competition in the near-wake. *J. Fluid Mech.* **191**, 225–245.

ROSHKO, A. 1954 On the drag and shedding frequency of two-dimensional bluff-bodies. *NACA Tech. Note* 3169, pp. 1–29.

SAFFMAN, P. G. & SCHATZMAN, J. C. 1982 An inviscid model for the vortex-street wake. *J. Fluid Mech.* **122**, 477–486.

SARPKAYA, T. 1978 Fluid forces on oscillation cylinders. *J. Waterways, Ports, Coastal Ocean Div. ASCE* **104**, 275–290.

SARPKAYA, T. 1979 Vortex-induced oscillations – a selective review. *Trans. ASME* E: *J. Appl. Mech.* **46**, 241–258.

SREENIVASAN, K. R. 1985 Transition and turbulence in fluid flows and low-dimensional chaos. In *Frontiers in Fluid Mechanics* (ed. S. H. Davis & J. L. Lumley), pp. 41–67. Springer.

STAUBLI, T. & ROCKWELL, D. 1988 Pressure fluctuations on an oscillating trailing edge. *J. Fluid Mech.* **203**, 307–346.

STEINER, T. R. & PERRY, A. E. 1987 Large-scale vortex structures in turbulent wakes behind bluff-bodies. Part 1. Vortex formation. *J. Fluid Mech.* **174**, 233–270.

TOEBES, G. H. & EAGLESON, P. S. 1961 Hydroelastic vibrations of flat plates related to trailing-edge geometry. *Trans. ASME* D: *J. Basic Engng* 671–678.

TRIANTAFYLLOU, G. S., TRIANTAFYLLOU, M. S. & CHRYSSOSTOMODIS, C. 1986 On the formation of vortex streets behind circular cylinders. *J. Fluid Mech.* **170**, 461–477.

UNAL, M. F. & ROCKWELL, D. 1988*a* Vortex formation from a cylinder. Part 1. The initial instability. *J. Fluid Mech.* **190**, 491–512.

UNAL, M. F. & ROCKWELL, D. 1988*b* Vortex formation from a cylinder. Part 2. Control by wake interference. *J. Fluid Mech.* **190**, 513–529.

VAN ATTA, C. W. & GHARIB, M. 1987 Ordered and chaotic vortex streets behind circular cylinders at low Reynolds numbers. *J. Fluid Mech.* **174**, 113–133.

WILLIAMSON, C. H. K. & ROSHKO, A. 1988 Vortex formation in the wake of an oscillating cylinder. *J. Fluids Struct.* **2**, 355–381.

WOOD, C. J. 1971 The effect of lateral vibrations on vortex shedding from blunt based aerofoils. *J. Sound Vib.* **14**, 91.

ZDRAVKOVICH, M. M. 1977 Review of flow interference between two circular cylinders in various arrangements. *Trans. ASME* I: *J. Fluids Engng* **99**, 618–633.